

UFG Cu bonding

Krishnamurty Balasubramanian

Related papers

[Download a PDF Pack](#) of the best related papers 



[Microstructure stability of ultra-fine grained magnesium alloy AZ31 processed by extrusion a...](#)

Miloš Janeček, Josef Stráský

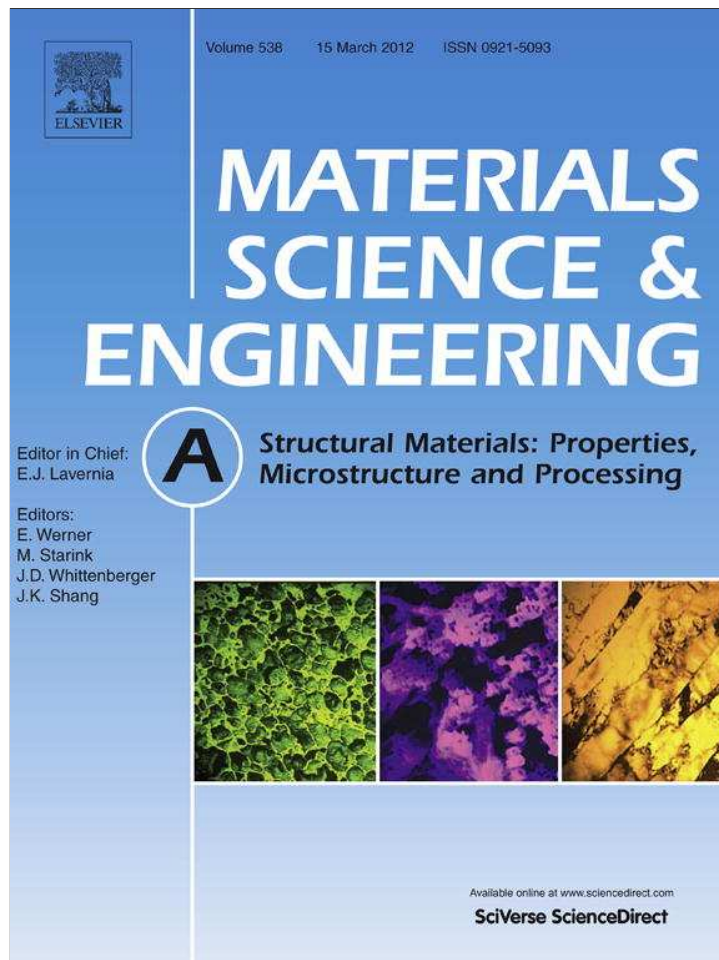
[Texture, microstructure and mechanical properties of equiaxed ultrafine-grained Zr fabricat ed by acc...](#)

Patric Gruber

[A Portrait of Copper Processed by Equal Channel Angular Pressing](#)

Miloš Janeček

Provided for non-commercial research and education use.
Not for reproduction, distribution or commercial use.



This article appeared in a journal published by Elsevier. The attached copy is furnished to the author for internal non-commercial research and education use, including for instruction at the authors institution and sharing with colleagues.

Other uses, including reproduction and distribution, or selling or licensing copies, or posting to personal, institutional or third party websites are prohibited.

In most cases authors are permitted to post their version of the article (e.g. in Word or Tex form) to their personal website or institutional repository. Authors requiring further information regarding Elsevier's archiving and manuscript policies are encouraged to visit:

<http://www.elsevier.com/copyright>



Contents lists available at SciVerse ScienceDirect

Materials Science and Engineering A

journal homepage: www.elsevier.com/locate/msea

Recrystallisation and bonding behaviour of ultra fine grained copper and Cu–Cr–Zr alloy using ECAP

P.K. Jayakumar^{a,*}, K. Balasubramanian^a, G. Rabindranath Tagore^b

^a Nonferrous Materials Technology Development Center, Hyderabad 500058, AP, India

^b National Institute of Technology, Warrangal 506004, AP, India

ARTICLE INFO

Article history:

Received 22 October 2011

Accepted 12 December 2011

Available online 14 January 2012

Keywords:

Equal channel angular processing

Cu–Cr–Zr alloy

Microstructure

Electron microscopy

Diffusion bonding

ABSTRACT

The structure, thermal stability and diffusion bonding behaviour of oxygen free high conductivity copper (OFHC), and Cu–Cr–Zr alloy (CRZ) with ultra fine grains (UFG) produced by severe plastic deformation through equal-channel angular pressing (ECAP) are investigated. Microstructural study reveals a grain refinement from 150 μm to 200 nm sized grains after 8 ECAP passes. Thermal stability of ECAP processed OFHC and CRZ has been investigated. Both OFHC and CRZ show hardness reduction at temperatures above 100 °C. However CRZ exhibits grain size stability up to a temperature of 500 °C. Diffusion bonding studies reveal that bond strengths of ~ 54 MPa are developed between ECAP processed CRZ and OFHC at a lower temperature of 500 °C when compared to annealed materials.

© 2011 Elsevier B.V. All rights reserved.

1. Introduction

ECAP process is the most viable forming process to extrude material using specially designed channel dies without substantial change in geometry resulting in ultra fine grained (UFG) materials [1–3]. The possibility to produce massive UFG specimens via severe plastic deformation makes them attractive for engineering applications and creates new opportunities to explore their specific properties in comparison with ordinary coarse grain materials using the standard specimens. Equal-channel angular pressing (ECAP) [2,3] is a technique that allows us to achieve extremely large imposed strains through intensive simple shear in bulk samples. The properties of the materials are strongly dependent on the plastic deformation behaviour during pressing that is governed mainly by die geometry (channel angle, corner angle and preform geometry), material properties (strength and hardening behaviour), and process variables (temperature and lubrication). However, many modern engineering applications require a rather sophisticated combination of physical and mechanical properties. Therefore joining aspect of the UFG materials is of high technological importance. Diffusion bonding characteristics of the material mainly depend on the thermal stability and recrystallisation behaviour of the UFG. In this paper, focus of the study is thermal stability and bonding behaviour of the UFG materials. Large number of literature is available on the grain refinement of OFHC during ECAP processing [4–7].

Dalla Torre et al. [6] has summarised the various reported grain refinement data of OFHC copper (after various ECAP passes). Lugo et al. [7] has reported the poor thermal stability and fast recrystallisation of ECAPed OFHC at substantially low temperatures (~ 200 °C).

Copper chromium zirconium alloys have been used in variety of application including electrode lugs, nuclear fusion reactor components, because of their vacuum compatibility, thermal, electrical and mechanical properties and their excellent stability at higher temperatures (200–400 °C). This alloy is traditionally used in applications where a combination of high mechanical strength, heat resistance and electrical (or thermal) conductivity is demanded (electrodes for micro point welding, heat exchangers, fusion reactors, etc.). One of the most effective methods of achieving higher mechanical strength is grain refinement by severe plastic deformation (SPD). CRZ is a precipitation hardenable alloy with high aging response in 450–600 °C temperature range. A comprehensive description on effect of time and temperature on the precipitation hardening is available in the relevant literature [8–14]. Vinogradov et al. [14], presented a detailed study on the thermal stability of aged and ECAPed samples of CRZ. However there are few published data on thermal stability of ECAPed Cu–Cr alloys [14,15].

2. Experimental procedure

OFHC copper and Cu–Cr–Zr alloy rods of 10 mm diameter are used as deformable material for the study. Cold drawn OFHC (99.99% pure) rods of 10 mm diameter were annealed at 600 °C for 2 h in vacuum to obtain a hardness of 80 HV and a grain size of 120–150 μm . Before ECAP the CRZ billet (Cu–0.44Cr–0.2Zr the

* Corresponding author. Tel.: +91 4024340592; fax: +91 4024340592.
E-mail address: pkjay@gmail.com (P.K. Jayakumar).

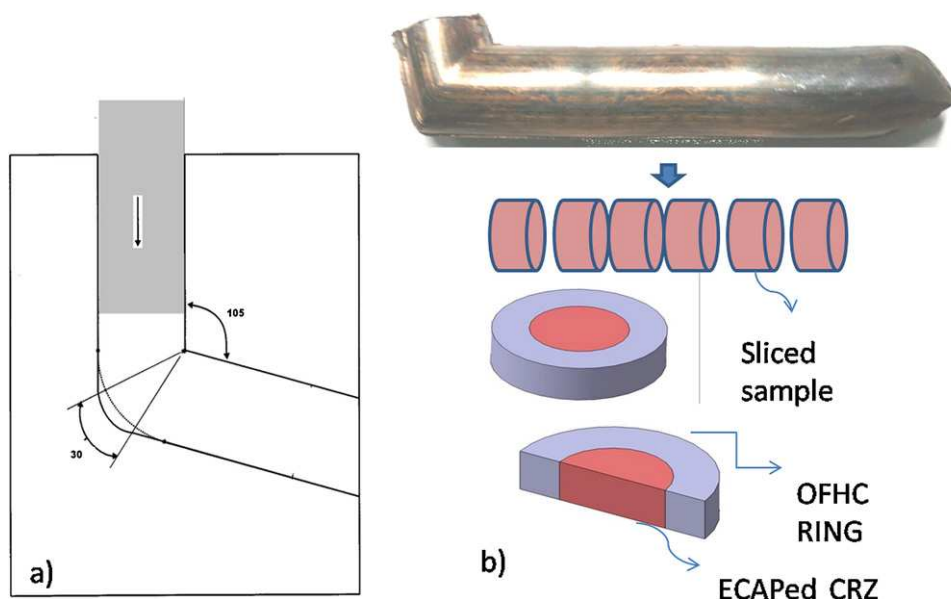


Fig. 1. (a) ECAP schematic and (b) diffusion bonding schematic of ECAP processed samples.

concentration of alloying elements is given in wt.%) of 10 mm was solution treated at 940 °C for 30 min and quenched in 5% brine.

After quenching, the samples were found to have hardness of 100 HV and a grain size of 40–80 μm . ECAP multiple pressing was performed (around 1–4 times for CRZ and 1–8 times for OFHC) with 1 mm/s velocity at room temperature via route Bc (the billet is rotated 90° CW around the longitudinal axis between consecutive passes) using a die set with circular channels that intersect at an angle $\Phi = 105^\circ$ and an outer arc angle $\Psi = 30^\circ$ as shown in Fig. 1a. This configuration imparts a strain of ~ 0.88 with low inhomogeneity in strain with each ECAP pass.

With the exception of the entry and exit points, the channel diameter was uniformly 10 mm. The diameter was slightly enlarged at the entry and exit points to permit easy reinsertion of the sample in the channel. The initial samples of OFHC were cut into billets of 6.5 cm length and 9.8 mm diameter that permitted a loose fit in the channel. Pressing was carried out using H-13 tool steel plunger guided by a hydraulic press. The tolerance of the plunger was kept extremely low to prevent material from flowing between the walls of the channel and the plunger.

Mechanical property data at room temperature was obtained from all ECAPed specimens from microhardness measurement as well as compression testing, using universal testing machine (Shimadzu 250UTM). The Vickers hardness was measured on the plane perpendicular to the working direction in the as-fabricated ECAP state after different number of pressings through the dies and after annealing under various conditions. The applied load was 500 g, and the loading time was of 15 s. The average values of at least five successive measurements were calculated. Grain size determination of the ECAPed samples was carried out through several micrographs taken from optical microscope and transmission electron microscope (TEM).

Thermal stability studies were carried out on 5 mm thick disks, cut from ECAPed samples (Fig. 1b). After 2 pass Bc ECAP deformation, isochronal annealing was carried out on select samples at various temperatures ranging from 80 to 300 °C. Set of samples after ECAP processing from 1 to 4 passes were held at various temperatures for 10 min duration. Hardness measurements were made on each sample after isochronal annealing. Recrystallisation effects were investigated by subjecting the ECAP processed samples to isothermal annealing. The samples were subjected to isothermal

annealing at six different temperatures (between 100 and 600 °C for OFHC, and 300 and 900 °C for CRZ).

Microstructural examinations were made on each sample after isothermal annealing.

Diffusion bonding was carried out between 10 mm diameter, 5 mm high CRZ samples and 10 mm ID and 17.5 mm OD and 5 mm high OFHC rings as shown in Fig. 1b. In order to study the effect of ECAP process on diffusion bonding, samples were selected from OFHC after 2 pass Bc and CRZ after 2 pass Bc. These samples were joined to fully annealed samples of OFHC ring. A third set of bonding was carried out between fully annealed OFHC and solution annealed CRZ ring. Diffusion bonding between CRZ and OFHC were carried out by heat treating the assembled sample at various temperatures ranging from 400 to 900 °C, whereas the bonding between OFHC and OFHC rings were carried out at temperatures ranging from 200 to 600 °C. Trials were carried out for a soaking time of 30 min. In order to evaluate the strength of the bond, a type of shear loading test was developed in accordance with F 1044-87 ASTM.

3. Results and discussion

3.1. Mechanical testing

Fig. 2a shows the Vickers hardness behaviour of OFHC copper as a function of number of passes. As it can be clearly seen, hardness saturates after 4 passes. These results are in reasonable agreement with different researchers [4,5]. If one applies Hall–Petch relation rough estimate of the grain size can be obtained. The grain size estimated from Hall–Petch relation using the yield stress values (Fig. 2b) is listed in Table 1. There is some variation in the

Table 1
Calculated grain sizes from the Hall–Petch relationship.

References	k (MPa $\text{m}^{1/2}$)	d (grain size)
Gourdin and Lassila [16]	0.278	382 nm
Wang and Murr [17]	0.58	1.6 μm
Hayashi et al. [18]	0.249	308
Andrade et al. [19]	0.056–0.26	334 nm
Armstrong [20]	0.11	60 nm

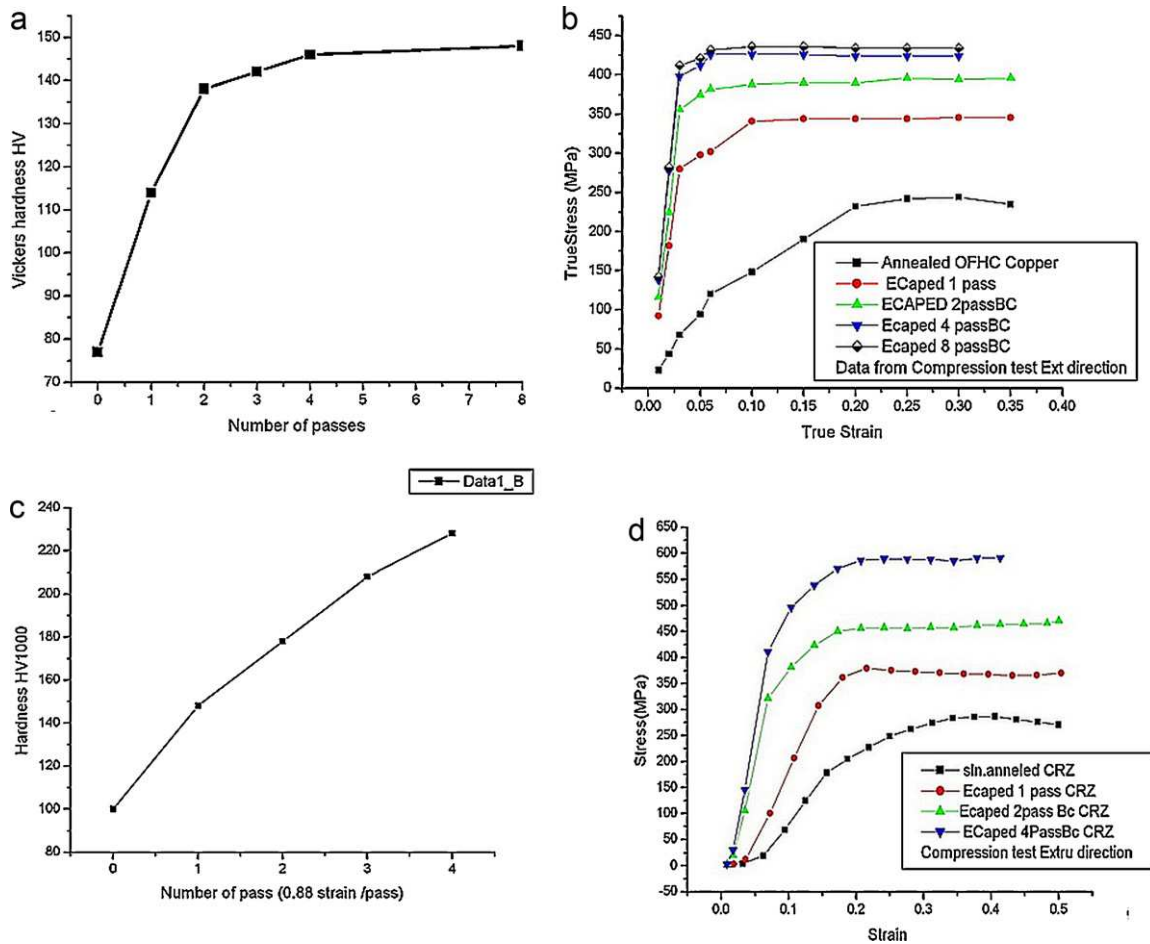


Fig. 2. Mechanical test results: (a) plot of hardness as function of number of passes from OFHC samples; (b) compression test results from 1 to 8 pass Bc OFHC; (c) plot of hardness as function of number of passes from CRZ samples; (d) compression test results from 1 to 4 pass Bc CRZ.

Hall–Petch slope in the literature [16–20], and the values are presented in Table 1. The results of compression tests are presented in Fig. 2b. The two-pass sample showed a significant jump in strength over the initial sample. The rise in strength with subsequent passes was not as significant as it was for the first two passes. This is suggestive of the fact that the most bulk of grain refinement happens in the first few passes only. ECAP yielded a steep decline in the grain size down to 500 nm (lamellar band spacing) on the first few passes while additional passes simply reduced the grains to ~200 nm size range. It was also observed that the effect of initial state of specimen (grain size inhomogeneity) did not affect the mechanical response significantly. After two passes, the effects of the initial inhomogeneous microstructure are essentially eliminated.

CRZ shows higher strain hardening when compared to OFHC (CRZ reaching a hardness of 228 HV (Fig. 2c) after 4 pass Bc). The results of compression tests are presented in Fig. 2d. Unlike OFHC, CRZ shows a continuous improvement in strength after subsequent passes with the 4 pass Bc ECAPed material, reaching a yield strength of 554 MPa. These results are in good agreement with published results [14,15].

3.2. Microstructure

The microstructure of the annealed OFHC (before ECAP) consists of equiaxed grains with an average size of 150 μm and some twinning. The microstructures of the ECAP samples processed from

1 to 8 passes through the die are illustrated in Fig. 3a–g. ECAP specimens were examined by TEM as well as optical microscope in the longitudinal (along the extrusion) and transverse (perpendicular to extrusion) directions. The microstructures after 0, 2, 4, 6 and 8 passes using route Bc are shown in Fig. 3a–f. It is found that the single pass leads to substantial reduction in grain size and the microstructure bands of subgrains and as demonstrated by the selected area diffraction pattern (SAD) after two pass the grain boundaries have low angles of misorientation. The grain size, measured by the linear intercept method shows grain size (lamellar boundary spacing) reducing to $\sim 0.5 \mu\text{m}$ after first pass, the spacing found to be reducing to $\sim 200 \text{ nm}$ with consecutive passes. After four passes more homogeneous equiaxed subgrain structures are found. However as the SAD pattern shows large presence of grains with low angled boundaries. No marked improvement in the average grain size was observed in the consecutive passes ($\sim 250 \text{ nm}$). After six passes the more equiaxed grains were found when compared to elongated grains. The lamellar boundary structure formed in first few passes are truncated by different shear planes during the consecutive passes [4]. After eight passes, some areas still show remnant elongated grains, although the proportion of equiaxed subgrains is large. The SAD pattern from eight pass samples (Fig. 3g) show angular spread of the spots indicating presence of large number of grains with high angled boundaries. The microstructural observations are typical of ECAP of pure copper [4–8] and are in good agreement with the mechanical test results.

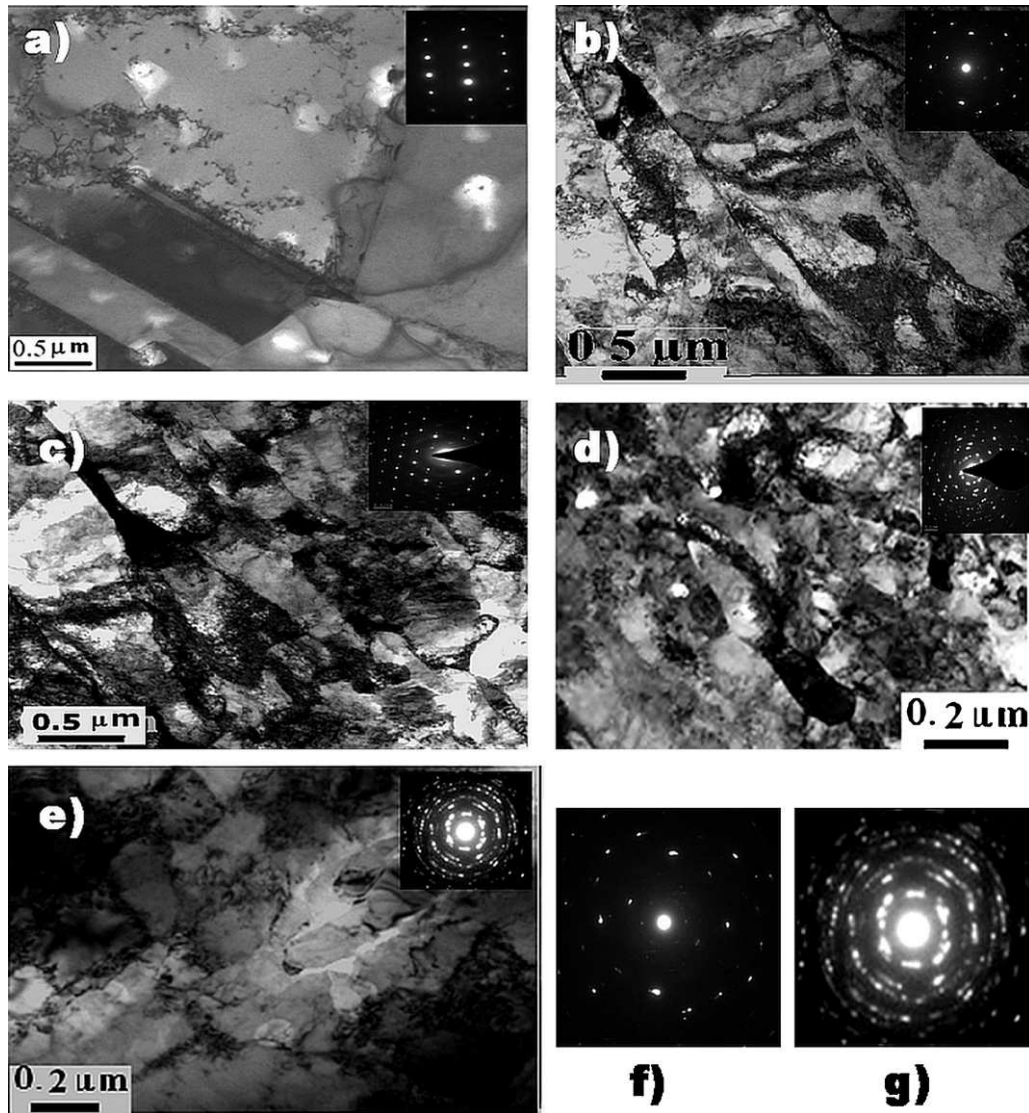


Fig. 3. Microstructure of ECAPed OFHC after different passes: (a) annealed condition 0 pass; (b) after ECAP 2 pass Bc; (c) after ECAP 4 pass Bc; (d) after ECAP 6 pass Bc; (e) TEM after ECAP 8 pass Bc; (f) SAD pattern after 2 pass; (g) SAD pattern after 8 pass.

The microstructure of the solution annealed CRZ (before ECAP) as shown in Fig. 4a, consists of equiaxed grains with an average size of $100\ \mu\text{m}$. TEM images from 1, 2 and 4 pass ECAP samples are given in Fig. 4 along with SAD patterns. ECAP results in a significant microstructure refinement. The microstructure mainly consists of deformed elongated grains with a width of $\sim 0.6\ \mu\text{m}$, which are delineated by dense dislocation wall. The cells are elongated in shape in the consecutive passes also. Their boundaries consist of dislocation bundles and have low misorientation angles. Equiaxed grains are visible in pass four samples with an average grain size of $\sim 0.4\ \mu\text{m}$. Such a microstructure is typical for conventional deformation of Cu based alloys. Different from OFHC, the ECAP of CRZ reveals microstructure with high dislocation density. The boundaries have diffuse appearance; these should be low-angle boundaries. Many dislocations appear both at grain boundaries and inside grains as shown in Fig. 4b and d. The higher strain hardening properties of CRZ may be attributed to the fact that CRZ structures are strengthened by the large accumulated dislocations in the grains. Microstructural observations are in good agreement with published literature ECAP of solution treated Cu–Cr alloys [14,15,21–23].

3.3. Annealing details

Hardness measurements carried out on samples after isochronal annealing are shown in (Fig. 5a and b). OFHC shows a decrease in hardness above $150\ ^\circ\text{C}$ isochronal annealing for samples ECAP processed with two passes whereas for higher passes the decrease in hardness was observed at lower temperature of $100\ ^\circ\text{C}$. Recrystallisation starts at lower temperature with increase in number of passes. Irrespective of the number of passes, a similar microstructure evolution could be observed during annealing characterized by the appearance of new larger grains in the deformed structure (Fig. 6a–d). In the course of annealing, the fraction of these larger grains grew at the expense of the deformed microstructure, and this proceeded faster with increasing number of ECAP passes. Hardness response to annealing cycle has similar results as reported by other investigators [7,24]. CRZ follows similar behaviour with hardness reduction initiated at a low temperature $80\ ^\circ\text{C}$ after 4 pass Bc (Fig. 5b). However, the hardness properties were found to be reducing with increase in soaking temperature. Above $600\ ^\circ\text{C}$ the CRZ samples showed similar grain growth as that of OFHC samples with the grain size reaching $100\ \mu\text{m}$ after $900\ ^\circ\text{C}$ heat

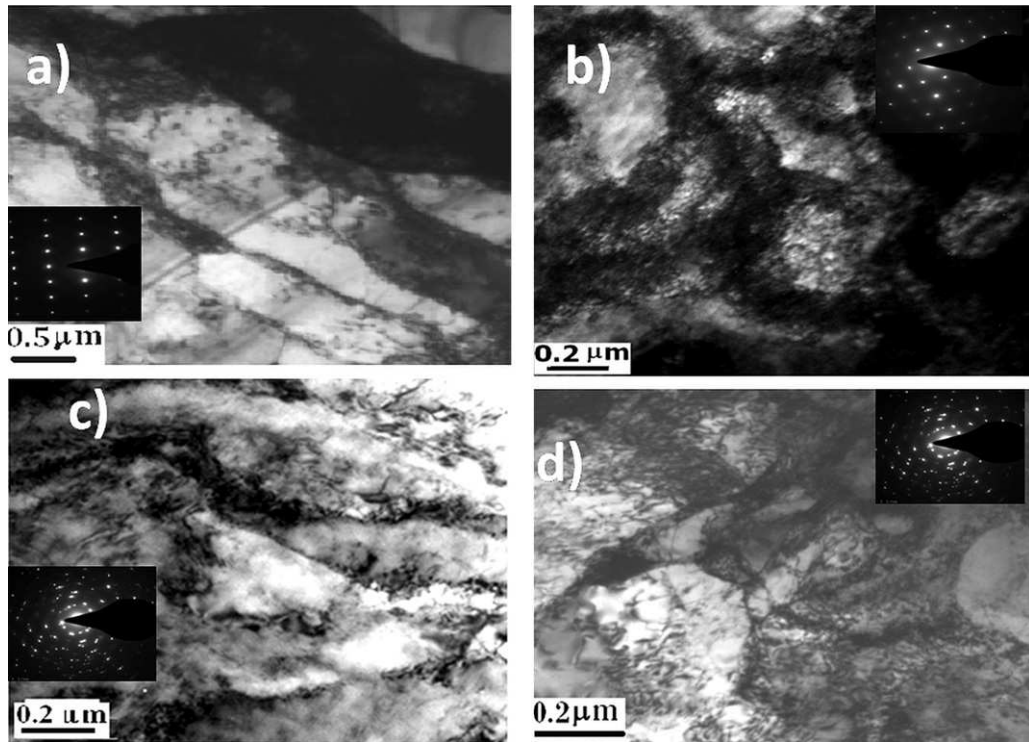


Fig. 4. Microstructure of ECAPed CRZ samples after different passes with inset SAD patterns (a) after 1 pass; (b) after 2 pass Bc; (c and d) TEM after 4 pass Bc.

treatment. The thermal stability (in grain size) of ECAPed CRZ up to 500 °C has been substantiated by other investigators [14]. This may be the reason for higher residual hardness after isochronal annealing at different temperatures below 500 °C. Above 500 °C temperature the strength of CRZ is influenced by the precipitation process.

Microstructural examination of the ECAPed OFHC samples annealed at temperatures from 100 to 500 °C is shown in Fig. 6. Significant changes in grain size and aspect ratio were observed at higher temperature heat treatment.

An increase in grain size was observed after heat treatment to a temperature of 300 °C, irrespective of the number of passes given to the specimen. However, heat treatments at temperatures higher than 400 °C, exhibit rapid and heterogeneous grain growth. Fig. 6c and d shows the microstructures of samples after the annealing at 400 and 600 °C under severe strain conditions of the ECAPed samples.

It is to be noted that the ECAP processed CRZ the structure remains fine-grained during heating and aging at temperatures up to 500 °C, as shown in Fig. 6e and f. No substantial grain growth

is noticed. Fig. 6f–h shows the microstructural details of the ECAP processed samples treated at 500, 600 and 900 °C. Figs. 6f and 7a show the cell structure as obtained from the samples after ECAP and heat treatment at 500 and 250 °C exhibits only recovery (reduction in hardness as shown in Fig. 5b) without any significant recrystallisation. Microstructure after 250 °C annealing as shown Fig. 7a, shows the grain size remain unaffected with most of the grains free of dislocation. It may be noted that for CRZ heat treatment between 450 and 600 °C results in precipitation of Cr from the solid solution resulting in strong pinning of grain boundaries [14]. The mechanical properties shall therefore depend on the precipitation hardening of the CRZ hardening. The grain growth becomes note worthy only at heat treatment temperatures higher than 600 °C.

The precipitation hardening response to heat treatment is appreciable only for treatment process above 450 °C and for longer time durations (>1 h) and HT below 450 °C results in fall in hardness properties as reported by various investigators [9,10]. Fig. 7 shows the TEM images from HT samples below 250 °C and HT samples at 600 °C. Fig. 7a (below 250 °C heat treated sample) shows

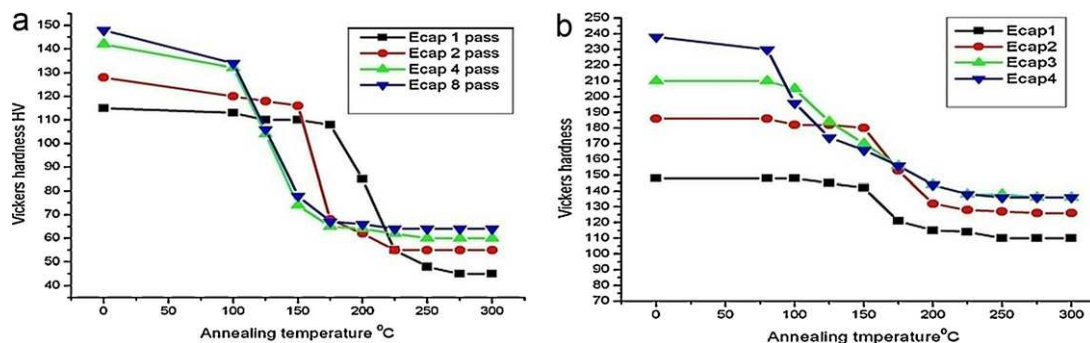


Fig. 5. Hardness values after isochronal annealing at different temperatures (30–300 °C). (a) ECAPed OFHC samples with 1, 2, 4 and 8 passes; (b) ECAPed CRZ samples with 1–4 passes.

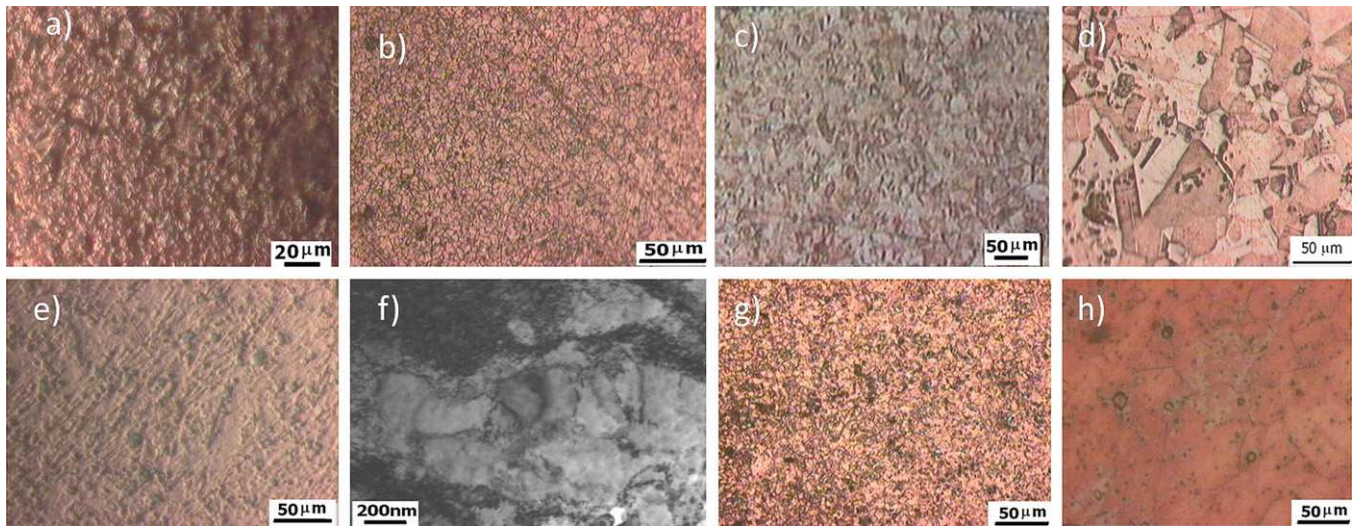


Fig. 6. Microstructure of samples from annealing study: (a) OFHC after ECAP 2 pass Bc at room temperature; (b) OFHC after ECAP 2 pass Bc and annealing at 200 °C; (c) OFHC after ECAP 2 pass Bc and HT at 400 °C; (d) OFHC after ECAP 2 pass Bc and HT at 600 °C; (e) CRZ after ECAP 2 pass Bc at room temperature; (f) CRZ after ECAP 2 pass Bc and HT at 500 °C; (g) CRZ after ECAP 2 pass Bc and HT at 600 °C; (h) CRZ after ECAP 2 pass Bc and HT at 900 °C.

no marked presence of precipitate particle in the microstructure, that are found in large number across the microstructure of above 600 °C aged sample (Fig. 7b).

3.4. Diffusion bonding

Electron microscopy image at the interface of the bond formed at 500 °C shows void free coalescence of the two materials (Fig. 8a). As shown in Fig. 8b, energy dispersive X-ray (EDX) line scan analysis of chromium across the interface reveals poor diffusion of chromium from CRZ region to OFHC region. Bond strength is tested using UTM with a 9 mm diameter plunger giving shear force as shown in Fig. 8c. The details of the test results are plotted as shown in Fig. 8d. The joint samples between ECAPed OFHC and OFHC ring showed increased bond strengths with increase in soaking temperatures. These studies were conducted up to a temperature of 600 °C. OFHC–ECAPed CRZ joint shows no bond/poor bond up to a temperature of 500 °C. It may be noted that the mechanical locking of the ring and ECAPed disc itself give shear resistance of 1–4 MPa. The joint strength of samples treated below 500 °C was less than 5 MPa and the results were inconsistent, indicating that no bond/poor bond is developed between ECAPed CRZ and annealed OFHC ring. Above 600 °C diffusion bonding resulted in similar improvement in bond strength with bonds formed at 900 °C reaching a bond

strength of 65 MPa. The fully annealed sample set (OFHC–CRZ SIn) shows poor/no bond up to a soaking temperature of 700 °C. It may be noted that there is substantial improvement in bond strength of joints formed of pre-ECAPed samples when compared to the fully annealed combinations.

Various investigators have established the stored energy increase in copper grains and the lowering of recrystallisation temperature with increase in number of ECAP passes [7,25]. Zhang et al. [25] have shown that with increase in strain (number of ECAP passes) the stored energy in the copper increases. These values are as high as 45 J/mol for two passes and reach a maximum of 55 J/mol after 8 passes. Further it may be noted that in the first few passes there is sharp increase in stored energy when compared to the subsequent passes and the value saturates around 55 J/mol after 8 number passes. This stored energy dependency and consequent lowering of recrystallisation temperature is established in the work reported [7,25]. The authors have reported the fall in recrystallisation temperature to 260 °C after first pass itself. With the subsequent passes the recrystallisation temperature falls to 210 °C. As the stored energy saturates after 8 pass, there is no further reduction in recrystallisation temperature. It may be noted that for a 2-pass sample, the stored energy is as high as 45 J/mol and the corresponding recrystallisation temperature is less than 250 °C. The diffusion bonding mechanism is enhanced by the

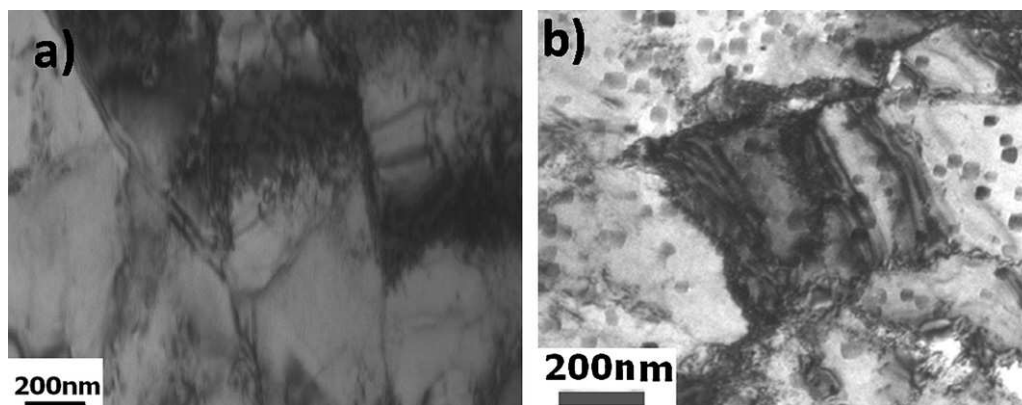


Fig. 7. Microstructure showing precipitation effects in heat treatment (a) below 250 °C and (b) HT at 600 °C showing precipitates (dark spots).

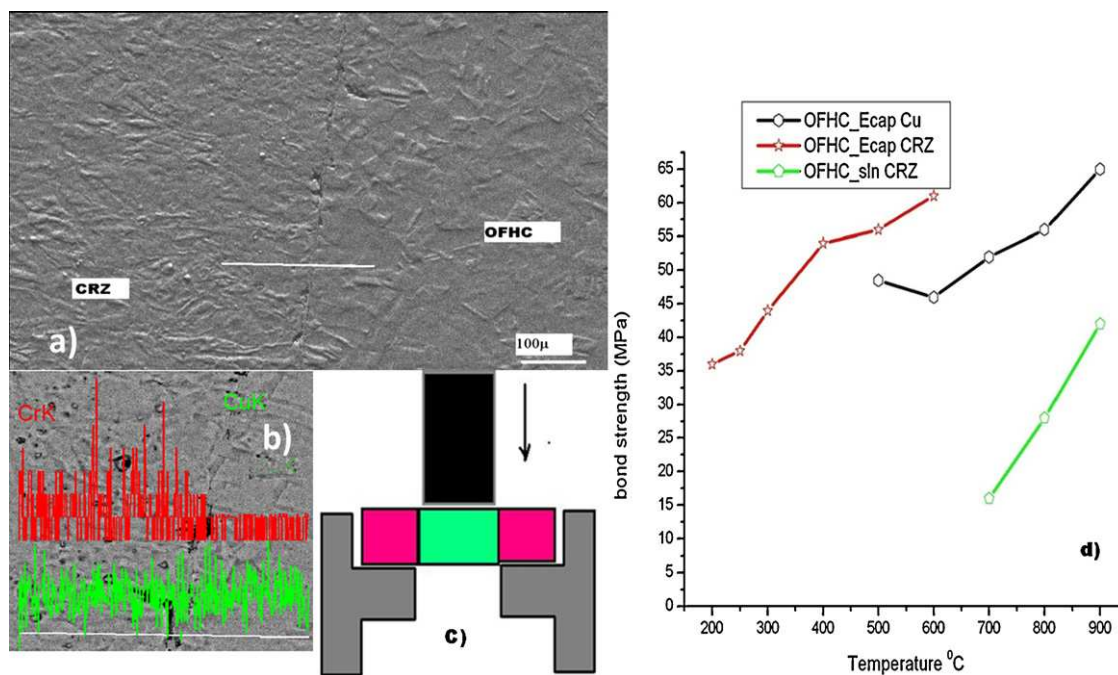


Fig. 8. (a) SEM micrograph at interface of CRZ–OFHC diffusion bond, (b) EDX line scan at interface, (c) bond strength test set up schematic and (d) bond strength results from diffusion bonded samples.

stored energy in the highly strained ECAP processed copper. This gives the explanation for improved bond strength of the ECAPed samples when compared to annealed samples.

4. Conclusion

The acquired mechanical strength in ECAP processes disappears due to the fast recrystallization and grain growth phenomena. Annealed OFHC samples exhibited non-uniform grain morphologies and size distribution, CRZ exhibit higher thermal stability up to 500 °C compared to OFHC (<200 °C). The specific findings are summarised as follows:

1. Annealing studies (30–300 °C) show large reduction in mechanical properties of OFHC and CRZ. CRZ exhibit higher residual strength after annealing due to the stable UFG structure.
2. The diffusion bonding in the ECAPed materials is found to be influenced by the lowering of recrystallisation temperature due to the stored energy in structures during ECAP. Diffusion bonding studies show that higher bond strengths achieved at lower temperature diffusion process with ECAP processed materials.
3. Diffusion bonding in CRZ is limited by the poor recrystallisation below 500 °C; whereas the OFHC forms strong bonds due to the fast recrystallisation process in the ECAPed structures (>200 °C).

Acknowledgement

The authors are indebted to Dr. V.S. Raghunathan and Mr. N. Krishnamurthi (Central University of Hyderabad) for their skillful help in TEM observations.

References

- [1] V.M. Segal, *Mater. Sci. Eng. A* 197 (1995) 157.
- [2] R.Z. Valiev, R.K. Islamgaliev, I.V. Alexandrov, *Prog. Mater. Sci.* 45 (2000) 103–189.
- [3] T.G. Langdon, *Mater. Sci. Eng. A* 462 (2007) 3–11.
- [4] F. Dalla Torre, R. Lapovok, J. Sandlin, P.F. Thomson, C.H.J. Davies, E.V. Pereloma, *Acta Mater.* 52 (2004) 4819–4832.
- [5] A. Mishra, B.K. Kad, F. Gregori, M.A. Meyers, *Acta Mater.* 55 (2007) 13–28.
- [6] F.H. Dalla Torre, A.A. Gazder, E.V. Pereloma, C.H.J. Davies, *J. Mater. Sci.* 42 (2007) 9097–9111, doi:10.1007/s10853-006-1261-7.
- [7] N. Lugo, N. Llorca, J.J. Sunol, J.M. Cabrera, *J. Mater. Sci.* 45 (2010) 2264–2273.
- [8] G. Durashevich, R. Todorovic, A. Kostav, M. Arsenovich, Z. Ivanich, *J. Metall.* 24 (1998), 123.
- [9] Q. Liu, X. Zhang, Y. Ge, J. Wang, J.-Z. Cui, *Metall. Mater. Trans. A* 37 (2006) 233.
- [10] L.I.U. Ping, S.U. Juanhua, D.O.N. Qiming, L.I. Hejun, *J. Mater. Sci. Technol.* 21 (4) (2005) 475.
- [11] G. Durashevich, V. Cvetkovski, V. Jovanovich, *Metallurgija J. Metall.* (2002) 291.
- [12] P. Liu, B.X. Kang, X.G. Cao, J.L. Huang, H.C. Gu, *J. Mater. Sci.* 35 (2000) 1691–1694.
- [13] I.S. Batra, G.K. Dey, U.D. Kulkarni, S. Banerjee, *J. Nucl. Mater.* 299 (2001) 91–100.
- [14] A. Vinogradov, V. Patlan, Y. Suzuki, K. Kitagawa, V.I. Kopylov, *Acta Mater.* 50 (2002) 1639–1651.
- [15] K.X. Wei, W. Wei, F. Wang, Q.B. Du, I.V. Alexandrov, J. Hu, *Mater. Sci. Eng. A* 528 (3) (2012) 25.
- [16] W.H. Gourdin, D.H. Lassila, *Acta Metall. Mater.* 39 (1991) 2337.
- [17] S. Wang, L.E. Murr, *Metallography* 13 (1980) 203.
- [18] K. Hayashi, H. Etoh, *Metall. Trans. JIM* 309 (1989) 925.
- [19] M.A. Meyers, U. Andrade, A.H. Chokshi, *Metall. Mater. Trans. A* 26 (1995) 2881.
- [20] R.W. Armstrong, in: R.F. Bunshah (Ed.), *Advances in Materials Research*, Interscience, New York, 1971, p. 101.
- [21] X. Molodova, G. Gottstein, M. Winning, R.J. Hellmig, *Mater. Sci. Eng. A* 460–461 (2007) 204–221.
- [22] M. Kulczyk, B. Zysk, M. Lewandowska, K.J. Kurzydłowski, *Phys. Stat. Sol. A* 207 (5) (2010) 1136–1138.
- [23] A. Vinogradov, T. Ishida, K. Kitagawa, V.I. Kopylov, *Acta Mater.* 53 (2005) 2181–2192.
- [24] C.Z. Xu, Q.J. Wang, M.S. Zheng, J.W. Zhu, J.D. Li, M.Q. Huang, Q.M. Jia, Z.Z. Du, *Mater. Sci. Eng. A* 459 (2007) 303–308.
- [25] Y. Zhang, J.T. Wang, C. Cheng, J. Liu, *J. Mater. Sci.* 43 (2008) 7326–7330.